Supporting Information for Pyramids and cascades: a synthesis of food chain functioning and stability

Matthieu Barbier and Michel Loreau

February 6, 2019

Appendix S1

Contents

Empirical estimates for m

We used the extensive metabolic data from many sources listed in the Supplementary Information ofl Makarieva et al. [2008] as well as a table from White and Seymour [2003], and matched the listed taxa with the Global Biotic Interactions (GloBI) database [Poelen et al., 2014], either at the species or the genus level (results shown here correspond to matches at the genus level; 20% are also matches at the species level, restricting to these matches does not change the results significantly, see Fig. S6) Taxa were categorized in large classes following the labels of Tables S1 to S11 in [Makarieva et al., 2008]. We could thus compute metabolic ratio m across 11822 predator-prey and 150 parasite-host pairs, involving 2560 species in total. We also characterized the differences between top and intermediate predators in the 63127 tritrophic chains (50% within the same large taxonomic class, e.g. birds or fish in Fig. S3).

In particular, we found metabolic data for the predator-prey pair of *Sebastes caurinus* and *Ophiodon elongatus*, belonging to the same genera as some of the fish species in the kelp forest

study [Trebilco et al., 2016], and could thus estimate $m \sim 0.2$ for this pair, although this estimate is probably a lower-bound given the median $m \sim 1$ for piscivory (see Fig. S5) and the fact that metabolic data on the predator and prey may not have been obtained at the same life history stage, see the original data in FishBase [Froese and Pauly, 02/2018].

Chain equations

Let us assume that each trophic level is characterized by a given rate m_i that governs its growth, mortality and uptake, so we can write

$$\begin{aligned}\frac{1}{B_1}\frac{dB_1}{dt} &= m_1\left(g - DB_1\right) - m_2\alpha B_2,\\ \frac{1}{B_i}\frac{dB_i}{dt} &= m_i\left(-r - DB_i + \varepsilon\alpha B_{i-1}\right) - m_{i+1}\alpha B_{i+1}\end{aligned} \tag{S1}$$

with r, D and α simple scaling constants that are the same for all species (all differences between levels are now assumed to be contained in the rates m_i). We divide by Dm_i everywhere:

$$\begin{aligned}\frac{1}{Dm_1B_1}\frac{dB_1}{dt} &= 1 - B_1 - maB_2,\\ \frac{1}{Dm_iB_i}\frac{dB_i}{dt} &= -\frac{r}{D} - B_i + \varepsilon aB_{i-1} - maB_{i+1}.\end{aligned} \tag{S2}$$

Here $a = \alpha/D$ is the strength of interactions *compared to self-regulation* D, and m is the ratio of a predator's metabolic rate to its prey's. We retain the explicit expressions εa and ma to contrast a, which is a property of ecological interactions and dynamics, with ε and m, which can be characterized using physiological data.

Finally, notice that the carrying capacity of the basal level is $K = g/D$ in the absence of consumers. We can write the equilibrium condition of (S2) as

$$0 = -\rho - B_i + \varepsilon aB_{i-1} - maB_{i+1} \tag{S3}$$

with

$$\rho = \frac{r}{g}K \tag{S4}$$

If we want to compare the density-dependent and independent terms directly, we can choose to express all biomasses in units of the carrying capacity, so that $K = 1$, $\rho = r/g$. In that case, it is clear that $\rho > 1$ entails that metabolic costs are at least comparable to self-regulation (B_i in (S3), which is at most 1).

Derivation of the energetic formula

Our equilibrium equation (S3) admits as a special case the energetic formula discussed in the main text,

$$m_iB_i = Em_{i-1}B_{i-1} \qquad \Leftrightarrow \qquad 0 = -B_i + \frac{E}{m}B_{i-1}. \tag{S5}$$

It emerges in our model when we neglect both metabolic costs ($\rho \to 0$) and predation losses ($\lambda \to 0$). Comparing this and (S3) yields the identification

$$E = m\varepsilon a. \tag{S6}$$

Note that various works posit $E = \varepsilon$ [Jennings et al., 2007, Trebilco et al., 2013, Woodson et al., 2018], which only holds in the special case

$$a = 1/m \qquad \Leftrightarrow \qquad \alpha_{i,i-1} = Dm_{i-1}. \tag{S7}$$

We now explain more generally why self-regulation is needed to yield the proportionality between levels $B_i \propto B_{i-1}$ assumed in the energetic formula (S5). As discussed in the main text, the basic principle of the energetic paradigm is the proportionality of energy *fluxes* [Lindeman, 1942], i.e.

$$P_i \sim \varepsilon P_{i-1}. \tag{S8}$$

with P_i the biomass created per unit time.

To obtain a similar relation between B_i and B_{i-1}, we must find an allometric relationship $P_i \sim B_i^\gamma$ with some exponent γ. This allometric relationship can come from two sources: either it is imposed by the functional response, or it arises dynamically by the equality at equilibrium of growth (P_i) and losses (that scale with B_i).

This allometric scaling is however not necessarily present. In the dynamical paradigm, we have

$$P_i = F(B_i, B_{i-1}) \tag{S9}$$

with F the functional response. The Lotka-Volterra case gives

$$P_i = \varepsilon\alpha B_i B_{i-1} \tag{S10}$$

If we insert this into (S8), this gives

$$B_i B_{i-1} \sim \varepsilon B_{i-1} B_{i-2} \qquad \Rightarrow B_i \sim \varepsilon B_{i-2} \tag{S11}$$

Hence the flux equation in a Lotka-Volterra model entails a biomass proportionality between levels at a distance of 2, not between adjacent levels.

There are multiple ways to recover the energetic formula (S5) and the pyramidal structure $B_i \propto B_{i-1}$ in a dynamical context, and all involve some form of self-regulation. These ways include the following scalings, detailed below:

$$\begin{aligned} &P_i \sim B_i^2 && \text{(density-dependent mortality)},\\ &P_i \sim B_{i-1} && \text{(predator interference)},\\ &P_i \sim B_i && \text{(handling time)}. \end{aligned} \tag{S12}$$

We can see that inserting any of these into (S8) will then give the proportionality $B_i \propto B_{i-1}$.

The basic argument is that, from a dynamical perspective, the biomass at level $i-1$ does not immediately determine the biomass at level i. Instead, it induces growth in the consumers, until this growth is compensated by equal losses.

One option is for self-regulation to cause *losses* to *increase* sufficiently with B_i, via density-dependent mortality D_i. If we assume Lotka-Volterra functional response, $P_i = \varepsilon\alpha B_i B_{i-1}$, then the only way to get a classic pyramidal structure is if the dynamics eventually give rise to the scaling

$$P_i \sim B_i^2 \tag{S13}$$

We can interpret the left-hand side as a growth term, and the right hand side as a loss term; the two must be equal at equilibrium. Thus, losses must be proportional to B_i^2, i.e. they must arise from competition within level i. This is the assumption that has guided our choice of synthetic model, as it is the one for which we can most easily interpolate between bottom-up and top-down limits.

Another option is for self-regulation to cause *growth* to *decrease* sufficiently with B_i. This can be achieved with consumer interference: if

$$P_i = \varepsilon\alpha \frac{B_i B_{i-1}}{1 + I B_i} \tag{S14}$$

with I the interference term (see Discussion in main text), then in the limit of very large I,

$$P_i \sim B_{i-1} \tag{S15}$$

and the principle (S8) directly entails

$$B_{i-1} \sim \varepsilon B_{i-2}. \tag{S16}$$

This case is the one implicitly assumed by energetic models [Borgmann, 1987] which posit an allometric relation $P_i \sim B_{i-1}$.

A third option is a saturating (Type 2) functional response, representing predators that must spend time H handling each prey

$$P_i = \varepsilon\alpha \frac{B_i B_{i-1}}{1 + H\alpha B_{i-1}} \tag{S17}$$

In the limit of very large H, we then get $P_i \sim B_i$.

These three options seem very distinct, but they have similar equilibrium properties: they all entail a linear relationship between the biomasses of adjacent levels i and $i-1$ that is independent of other levels (because we can ignore either the biomass of levels above, as in interference and competition, or of levels below, as in Type 2 functional response).

Stability matrices

We detail here the statements in the main text on the equilibrium's stability properties, i.e. its response to various types of perturbations. As mentioned in Box 3, the dynamical equation (3) becomes

$$\begin{aligned} \frac{dB_i}{dt} =& B_i \left(g_i - D_i B_i + \varepsilon\alpha_{i,i-1} B_{i-1} - \alpha_{i+1,i} B_{i+1}\right) \\ &+ B_i \xi_i(t) \end{aligned} \tag{S18}$$

where $\xi_i(t)$ represents the perturbation.

A press perturbation $\xi_i(t) = \xi$ can be interpreted as a permanent change Δg_i in growth or mortality, which is why we chose in main text to emphasize $g_i = 0$ for $i > 0$ (low mortality limit $\rho = r/g \ll 1$) and suggest to represent the effects of higher mortality as the result of a press perturbation. Such a change in mortality shifts down the biomasses but preserves the qualitative shape of the distribution as long as r is moderate. Furthermore, it does not change the response to further press perturbations (due to linearity of equilibrium conditions in Lotka-Volterra equations) as long as all levels survive.

A stochastic perturbation will have a time-dependent $\xi_i(t)$, here scaled by B_i. In the case of demographic stochasticity resulting from random birth and death processes [Haegeman and Loreau, 2011], we expect the variance over time to be proportional to the abundance

$$\mathrm{Var}(B_i \xi_i) \sim B_i \tag{S19}$$

which corresponds to $\xi_i(t) = W(t)/\sqrt{B_i}$ with $W(t)$ a white noise term with mean 0 and variance 1.

In the main text, we focus on *relative* response, i.e. the fractional response $\Delta B_i/B_i$ to a press, or the coefficient of variation $\mathrm{std}(B_i)/B_i$ in response to noise. The corresponding matrices V in Fig. 3 and $C^{(i)}$ in Fig. 4 are computed as follows [Arnoldi et al., 2016]. Let A be the matrix

$$A_{ij} = (\varepsilon a \delta_{i-1,j} - ma\delta_{i+1,j} - \delta_{ij}) \frac{B_j}{B_i} \tag{S20}$$

where $\delta_{ij} = 1$ if $i = j$ and B_i, B_j are equilibrium abundances. The relative response to a press is the solution V of

$$AV = \mathbb{I} \tag{S21}$$

with $\mathbb{I}$ the identity matrix, i.e. $V = A^{-1}$.

To represent a white noise applied to species i only, we define a $S \times S$ matrix $\Sigma^{(i)}$ where all elements are zero except $\Sigma^{(i)}_{ii} = 1$. Then, the relative covariance matrix $C^{(i)}$ is the solution of the Lyapunov equation

$$AC^{(i)} + C^{(i)}A^T = \Sigma^{(i)}. \tag{S22}$$

The similarity of (S21) and (S22) reflects the connectedness between different stability properties.

Two levels: Control and production

Let us consider a two-level chain, where we allow each level to have a different self-regulation constant, so that we can explore the role of self-regulation independently at each level. At equilibrium,

$$\begin{aligned} 0 &= g - D_1 B_1 - m\alpha B_2 \\ 0 &= -r - D_2 B_2 + \varepsilon\alpha B1 \end{aligned} \tag{S23}$$

The solution is

$$\begin{aligned} B_1 &= \frac{m\alpha r + D_2 g}{D_1 D_2 + m\varepsilon\alpha^2} \\ B_2 &= \frac{\varepsilon\alpha g - r D_1}{D_1 D_2 + m\varepsilon\alpha^2}. \end{aligned} \tag{S24}$$

Top-down control and mortality

Without self-regulation, $D_1 = D_2 = 0$, it is well known, as shown in the main text (9), that each level is controlled by the other,

$$B_1 = \frac{r}{m\alpha}, \qquad B_2 = \frac{g}{\varepsilon\alpha} \tag{S25}$$

where B_1 depends on consumer mortality r, and B_2 depends on basal growth g.

If one level has self-regulation, but not the other (either $D_1 = 0$ or $D_2 = 0$), each species always plays an important role in controlling the other, as shown by the fact that $m\varepsilon\alpha^2$ (the absolute strength of the feedback through the other species) is present at the denominator in the biomasses of both levels. Intuitively, whichever level has no self-regulation will grow (pushing its consumers up or its resources down) until the top level consumes all extra basal growth and cannot grow further.

However, if *both* levels have self-regulation, $D_1, D_2 > 0$, consumers need not grow until they control resources.

In the limit of large D_2 (strong consumer self-regulation) i.e. when terms containing D_2 dominate all other terms in (S24), we find a situation of pure donor control. The expressions simplify to

$$B_1 \approx \frac{g}{D_1} \tag{S26}$$

i.e. the equilibrium biomass of the basal level is that of a simple logistic equation, ignoring all effects of consumption. On the other hand, for the consumer

$$B_2 \approx \frac{\varepsilon\alpha(g/D_1) - r}{D_2} \tag{S27}$$

and consumer mortality r simply acts as a negative press perturbation on the consumer.

Recall that without self-regulation, r controls resource biomass B_1, and is thus a crucial factor in functioning and stability patterns, such as trophic cascade strength. In (S27), r simply plays the role of a threshold for consumer survival (which requires $\varepsilon\alpha g > r D_1$) and does not impact lower levels.

Consumption-biomass relationships

Finally, let us discuss consumption-biomass relationships in this two-level system. In (S23) the fraction of production at level 1 removed by consumers is simply

$$f = \frac{m\alpha B_2}{g} = 1 - \frac{D_1 B_1}{g} \tag{S28}$$

Hence, we see that f is always 1 unless the basal level self-regulates $D_1 \neq 0$. We also find the relationship between f and the ratio of primary production to basal biomass, i.e. the basal energy influx g. Empirically [Cebrian and Duarte, 1994], it has been proposed that

$$f \sim g^{0.6} \tag{S29}$$

across aquatic and terrestrial plants. But we see here from a simple argument that this relationship might not be a power-law; rather, it may be a saturating curve that starts from zero when $g = B_1 D_1$, allowing us to estimate primary producer self-regulation D_1.

This simple relationship may, however, be modified in two ways. First, if g is tied to primary productivity p_1 but not equal to it, i.e. $g = p_1 - l$ with some losses l, then the true value $f \equiv m\alpha B_2/p_1$ may be smaller than the estimate (S28). Second, if herbivore biomass B_2 is significantly brought down by predation from a higher level, so that $m\alpha B_2 < g - D_1 B_1$, and in turn f will be smaller than the estimate (S28). In both cases, our estimate is thus an upper bound, and we may overestimate D_1 if we compute it from fitting this relationship.

Three levels: Trophic cascades

Let us now consider a three-level chain with different self-regulation coefficients, and let us also allow different metabolic rate ratios $m_{21} = m_2/m_1$ and $m_{32} = m_3/m_2$ (and thus $m_{31} = m_3/m_1$ can be defined for convenience).

We will further assume that α is fixed and independent of m, meaning that consumption is driven by consumer metabolism ($\alpha_{i,i-1} \sim m_i$).

The equilibrium is then

$$B_1 = \frac{1}{b}\left(g(D_2 D_3 + \alpha^2 \varepsilon m_{32}) + \alpha D_3 m_{21} r_2 - \alpha^2 m_{32} m_{21} r_3\right) \tag{S30}$$

$$B_2 = \frac{1}{b}\left(g D_3 \alpha \varepsilon + \alpha D_1 m_{32} r_3 - D_1 D_3 r_2\right) \tag{S31}$$

$$B_3 = \frac{1}{b}\left(g\alpha^2\varepsilon^2 - \alpha D_2 \varepsilon r_2 - (D_1 D_2 + \alpha^2 \varepsilon m_{21}) r_3\right) \tag{S32}$$

$$b = D_1 D_2 D_3 + \alpha^2 \varepsilon (D_1 m_{32} + D_3 m_{21}) \tag{S33}$$

Note that each level's biomass depends on basal productivity g only if higher levels (if they exist) are limited, either by self-regulation or by predation mortality.

Trophic cascades

To study the strength of trophic cascades, two distinct scenarios are conceivable. The first is to perform a press perturbation Δr_3 around equilibrium, increasing the mortality at the predator level $i = 3$, and compute the relative change $\Delta B_1/B_1$ as a response. The second is to remove the predator level altogether and compare biomass in a two-level chain $B_i^{(2)}$ to that in a three-level chain $B_i^{(3)}$. The general expressions are cumbersome, but enough intuition can be gathered from two special cases: self-regulation only happens at the bottom $D_2 = D_3 = 0$ (which is the most conventional choice in food web theory), or at the top $D_1 = D_2 = 0$.

Perturbations around equilibrium

In the case of a perturbation around equilibrium, we find

$$\left.\frac{\Delta B_1/B_1}{\Delta r_3}\right|_{D_2=D_3=0} = -\frac{1}{g/m_{21} - r_3} \tag{S34}$$

$$\left.\frac{\Delta B_1/B_1}{\Delta r_3}\right|_{D_1=D_2=0} = -\frac{\alpha m_{32}}{D_3 r_2 + m_{32}(\varepsilon g/m_{21} - r_3)} \tag{S35}$$

where the minus sign indicates that increasing mortality r_3 decreases basal biomass, as expected.

In both limits, the effect of basal growth g (and hence of enrichment) is to *reduce* cascade strength: looking more carefully, we see that in general

$$\frac{\Delta B_1}{\Delta r_3} = \frac{-\alpha^2 m_{32} m_{21}}{b} \tag{S36}$$

is independent of g, while B_1 increases with g, thus the relative change $\Delta B_1/B_1$ becomes negligible in the limit of high enrichment.

Note also that, if self-regulation only happens at the basal level $D_2 = D_3 = 0$, we do not expect cascade effects to increase with predator metabolism m_3 or decrease with herbivore metabolism m_2, as found empirically [Borer et al., 2005] (see main text). This prediction is, however, borne out in the case with predator self-regulation: the predator-plant metabolic ratio m_{31} is at the numerator, and the herbivore-plant ratio m_{21} is at the denominator.

Adding or removing a level

We next compute the ratio of basal biomass without predator to that with predator. In a two-level chain we have

$$B_1^{(2)} = \frac{m_{21}\alpha r_2 + D_2 g}{D_1 D_2 + m_{21}\varepsilon\alpha^2}$$

while in a three level chain we have (S30). Thus, we find

$$\left.\frac{B_1^{(3)}}{B_1^{(2)}}\right|_{D_2=D_3=0} = \alpha\frac{g\varepsilon - m_{21} r_3}{r_2 D_3} \tag{S37}$$

$$\left.\frac{B_1^{(3)}}{B_1^{(2)}}\right|_{D_1=D_2=0} = \frac{m_{32}}{m_{21}}\left.\frac{B_1^{(3)}}{B_1^{(2)}}\right|_{D_2=D_3=0} \tag{S38}$$

Here, the conclusion on the effect of enrichment appears opposite: high enrichment means low $\Delta B_1/B_1$ around equilibrium, but this also means high $B_1^{(3)}/B_1^{(2)}$, i.e. a large increase in biomass when adidng predators.

In general, enrichment can go either way: both $B_1^{(2)}$ and $B_1^{(3)}$ depend on g, and which dependence is faster (meaning how g influences cascade effects) is a function of all other dynamical parameters. The effect of enrichment can also disappear if D_2 and D_3 are both large, in which case both $B_1^{(3)}$ and $B_1^{(2)}$ are proportional to g and it cancels out of the ratio.

While the effect of enrichment is inconsistent, the role of metabolism remains similar to the case of smaller press perturbations: if $D_3 \neq 0$, we now expect the change in B_1 to increase linearly with $m_{32}/m_{21} = m_3 m_1/m_2^2$, and thus to be positively correlated with m_3 and anticorrelated with m_2, still in agreement with experimental conclusions. Note that this predicts that the log ratio $\log\left(B_1^{(3)}/B_1^{(2)}\right) \sim \log m_3 + \log m_1 - 2\log m_2$ decreases with m_2 twice as fast as it increases with m_3, also in agreement with empirical data [Borer et al., 2005].

Cascade attenuation or intensification

We can also compute how much the cascade effect of a perturbation around equilibrium is attenuated as it goes down the chain:

$$\frac{\Delta B_2}{\Delta B_1} = -\frac{D_1}{\alpha m_{21}} \tag{S39}$$

and thus the relative change

$$\begin{aligned}\frac{\Delta B_2/B_2}{\Delta B_1/B_1} &= -\frac{D_1 B_1}{\alpha m_{21} B_2} \\ &= 1 - \frac{1}{f_1}.\end{aligned} \tag{S40}$$

Thus, we can predict how much the cascade effect will be attenuated or amplified, depending on the fraction of removed production at level 1. When the data is given by log ratios [Hedges et al., 1999] such as

$$\Delta \log B_1 = \log\left(\frac{B_1^{(3)}}{B_1^{(2)}}\right) \tag{S41}$$

we can convert them to relative changes and back using

$$\Delta \log B_1 = \log\left(\frac{B_1 + \Delta B_1}{B_1}\right) \tag{S42}$$

$$\Delta B_1/B_1 = \exp(\Delta \log B_1) - 1. \tag{S43}$$

Pyramid slope

In the general chain, we have:

$$\frac{1}{B_i}\frac{dB_i}{dt} = \underbrace{m_i \varepsilon \alpha B_{i-1}}_{p} - \underbrace{m_{i+1}\alpha B_{i+1}}_{f_B} - \underbrace{m_i D B_i - m_i r}_{d} \tag{S44}$$

where p is productivity (the production/biomass ratio P/B), f_B is the fraction of biomass removed by predators per unit time (e.g. per day) [Cebrian and Duarte, 1994] and d is the remaining mortality term. Note that r may in fact have to be split into metabolic costs reducing productivity, and real mortality, which respectively enter into p and d.

The fraction of production removed is simply

$$f = \frac{f_B}{p} = \frac{m B_{i+1}}{\varepsilon B_{i-1}} = \frac{B_{i+1}}{\kappa B_{i-1}} \tag{S45}$$

which we easily interpret in the equilibrium condition (6) as the relative contribution of predation mortality among all the negative terms that balance out the positive biomass influx from consumption.

If $f = 1$ (strict top-down control), then $B_{i+1} = \kappa B_{i-1}$ and on average $B_i \sim \kappa^{i/2}$. More generally, if we assume a biomass pyramid with $B_{i+1} = u B_i$, we easily deduce from (6) with $r = 0$ that

$$\begin{aligned} u &= \sqrt{\kappa}\frac{\sqrt{1+4\lambda}-1}{2\sqrt{\lambda}} \\ u &\underset{\lambda\to 0}{\longrightarrow} \varepsilon a, \qquad u \underset{\lambda\to\infty}{\longrightarrow} \sqrt{\kappa}. \end{aligned} \tag{S46}$$

This simplified calculation from an ansatz $B_{i+1} = u B_i$ is made more precise below in the section "Explicit chain solution". Note that (S45) entails

$$u = \sqrt{\kappa f}, \tag{S47}$$

and hence we get the expression for the fraction of production removed by predators:

$$f = 1 - \frac{\sqrt{1+4\lambda}-1}{2\lambda}, \qquad \lambda = \frac{f}{(1-f)^2} \tag{S48}$$

and for the average biomass trend

$$B_i \sim u^i = (\kappa f)^{i/2} \tag{S49}$$

Finally, notice that the condition for linear mortality r to be negligible in d in (S44) is (using $D = g$ in our choice of units)

$$\frac{r}{g} \ll B_i \tag{S50}$$

If it is not negligible, then we find

$$\lambda = \frac{f}{(1-fR)^2}, \qquad R = 1 - \frac{r}{gamB_{i+1}} \tag{S51}$$

$$f = \frac{1}{R} - \frac{\sqrt{1+4\lambda R}-1}{2\lambda R^2} \tag{S52}$$

With high mortality, $R < 1$ and f is higher than expected from the low-mortality expression in the main text.

If r/g is a constant, in a regular pyramid, the condition $r/g \ll B_i$ will fail for upper levels more than for lower levels. Thus, low basal growth (low enrichment, high mortality) will tend to suppress top predators more and reduce cascades, in accordance with empirical intuitions [Pace et al., 1999].

Size spectrum exponents

The widely-used argument in the study of (especially marine) size spectra goes as follows: according to (1), the "energy content" $m_i B_i$ of a level depends on that of the level below:

$$m_i B_i \sim E m_{i-1} B_{i-1}.$$

Therefore

$$B_i \sim \frac{E}{m} B_{i-1} \tag{S53}$$

with m the predator-prey metabolic ratio, and

$$B_i \sim \left(\frac{E}{m}\right)^i. \tag{S54}$$

Now, following the argument in main text to express the trophic level i as a function of body size W

$$i \sim \frac{\log W}{\log M} \tag{S55}$$

with M the predator-prey mass ratio, and the allometric scaling

$$m \sim M^{-\beta} \qquad \Rightarrow \qquad \log m \sim -\beta \log M. \tag{S56}$$

Putting this all together, we find

$$\begin{aligned} B(W) &\sim e^{i \log(E/m)} \\ &= e^{\log W \dfrac{\log E + \beta \log M}{\log M}} \\ &= W^b, \qquad b = \beta + \frac{\log E}{\log M}. \end{aligned} \tag{S57}$$

Finally, some works [Trebilco et al., 2013, Woodson et al., 2018] assume that $E \approx \varepsilon$, i.e. the proportionality factor E is the real physiological conversion efficiency.

As we noted above, in our model $E = m\varepsilon a$, which can be larger than one, yielding an inverted energy pyramid. This is not a new result [Borgmann, 1987]. But it is important to note that $E = \lambda/a$, and a pyramidal biomass distribution (hence the energetic formula above) only occurs if $\lambda < 1$. Hence, $E > 1$ requires a small value of a. In the case of resource-driven consumption, as defined in the main text (Box 2), $a \sim 1/m$ and this could be achieved by having large m.

From our solution, we instead found in the main text

$$B(W) \sim W^b, \qquad b = \frac{1}{2}\left(\beta + \frac{\log \varepsilon f}{\log M}\right). \tag{S58}$$

This coincides with the above formula if

$$\lambda \ll 1, \qquad \Rightarrow f \approx \lambda = m\varepsilon a^2 \tag{S59}$$

In that case, $\varepsilon f \approx E^2/m$, hence

$$b \approx \frac{1}{2}\left(\beta + 2\frac{\log E}{\log M} - \frac{\log m}{\log M}\right). \tag{S60}$$

and since again $m \sim M^{-\beta}$, we recover the previous expression.

This calculation assumes that interaction strength a is independent from mass ratio M. However, see Fig. S7 for indications to the contrary, suggesting further corrections in the exponent b.

Explicit chain solution

Neglecting linear mortality, we can rewrite the equilibrium (6) as

$$B_{i+1} = -\sqrt{\frac{\kappa}{\lambda}}B_i + \kappa B_{i-1} \tag{S61}$$

If linear mortality is non negligible, then the same relation and all subsequent calculations hold for $\Delta B_i = B_i - B_{i-1}$ instead. The solution to this recurrence equation can be written as

$$B_i = c_+ B_+^i + c_- B_-^i \tag{S62}$$

where $c_\pm$ are two constants given by boundary conditions (basal growth and the top level), while the two roots of the characteristic polynomial are

$$B^\pm = \sqrt{\kappa}\frac{-1 \pm \sqrt{1+4\lambda}}{\sqrt{4\lambda}}. \tag{S63}$$

where it becomes apparent that

$$\begin{aligned} B_+ &= u = \sqrt{\kappa f} \\ B_- &= \sqrt{\frac{\kappa}{\lambda}} - B_+ = \frac{1}{ma} - u \end{aligned} \tag{S64}$$

according to our definitions above. Note the limits

$$B^+ \underset{\lambda\to 0}{\longrightarrow} \sqrt{\kappa\lambda} = \varepsilon a, \qquad B^+ \underset{\lambda\to\infty}{\longrightarrow} \sqrt{\kappa}$$

$$B^- \underset{\lambda\to 0}{\longrightarrow} \infty, \qquad B^- \underset{\lambda\to\infty}{\longrightarrow} -\sqrt{\kappa}$$

We can define a weighted average $\tilde{B}_i$ such that

$$\begin{aligned}\tilde{B}_i &= \frac{B_{i+1} - B_- B_i}{2} = \frac{B_{i+1} + B_i(\sqrt{\kappa f} - \sqrt{\kappa/\lambda})}{2} \\ &= c_+ B_+^i \frac{B_+ - B_-}{2} \\ &= c_+ (\kappa f)^{i/2} \sqrt{\frac{1}{4\lambda} + 1} \\ &\sim (\kappa f)^{i/2}. \end{aligned} \tag{S65}$$

In other words, both in the pyramid and the cascade regimes, there always exists a weighted average of consecutive levels, comprised between B_i (if $\lambda \ll 1$) and $B_i + B_{i+1}/\sqrt{\kappa}$ (if $\lambda \gg 1$) that will scale like $(\kappa f)^{i/2}$, thus giving general applicability to our conclusions on the biomass spectrum (19).

Body size dependence

The predator-prey ratio in metabolic rates m is an important parameter that could depend on organism body size. Metabolic scaling [Hemmingsen, 1960] suggests $m \sim M^{-\beta}$ with M the predator-prey body mass ratio. However, we show in Fig. S4 that this simple scaling makes erroneous predictions when compared to direct estimation of m for various interactions, in particular predicting the overall distribution of m to be skewed toward values smaller than 1 (as consumers are typically larger than their prey), while empirical distributions do not exhibit this skew – consumers have faster or slower metabolism depending on taxonomy, without a clear bias.

Furthermore, predator-prey metabolic ratio m might not be the only body size-dependent property. In particular, interaction strength (which enters a) may also vary with M. From data on kelp forest herbivores [Sala and Graham, 2002], we find that their predation effect on kelp, proportional to ma, decreases as $M^{-3/4}$ (see Fig. S7), significantly faster than the metabolic expectation $m \sim M^{-1/4}$. This suggests that the interaction strength decreases as

$$a \sim M^{-1/2}. \tag{S66}$$

If we still assumed that this arises from metabolic scaling, we could use (8) and obtain

$$a \sim m^\nu, \qquad \nu = \frac{1}{2\beta} \tag{S67}$$

an unexpected scenario with $\nu > 0$ (where we recall that dynamical models typically assume $\nu = 0$ and energetic models $\nu = -1$), i.e. consumption rate increasing superlinearly with consumer metabolism and decreasing with prey metabolism. Other physiological explanations based on size difference could thus be more plausible than a metabolic argument.

References

J.-F. Arnoldi, M. Loreau, and B. Haegeman. Resilience, reactivity and variability: A mathematical comparison of ecological stability measures. *Journal of Theoretical Biology*, 389:47–59, 2016.

E. Borer, E. Seabloom, J. Shurin, K. Anderson, C. Blanchette, B. Broitman, S. Cooper, and B. Halpern. What determines the strength of a trophic cascade? *Ecology*, 86(2):528–537, 2005.

U. Borgmann. Models on the slope of, and biomass flow up, the biomass size spectrum. *Canadian Journal of Fisheries and Aquatic Sciences*, 44(S2):s136–s140, 1987.

J. Cebrian and C. Duarte. The dependence of herbivory on growth rate in natural plant communities. *Functional Ecology*, 8(4):518–525, 1994.

R. Froese and D. Pauly. Fishbase, www.fishbase.org, 02/2018.

D. S. Glazier. Metabolic level and size scaling of rates of respiration and growth in unicellular organisms. *Functional Ecology*, 23(5):963–968, 2009.

B. Haegeman and M. Loreau. A mathematical synthesis of niche and neutral theories in community ecology. *Journal of Theoretical Biology*, 269(1):150–165, 2011.

L. V. Hedges, J. Gurevitch, and P. S. Curtis. The meta-analysis of response ratios in experimental ecology. *Ecology*, 80(4):1150–1156, 1999.

A. M. Hemmingsen. Energy metabolism as related to body size and respiratory surface, and its evolution. *Reports of the Steno Memorial Hospital (Copenhagen)*, 13:1–110, 1960.

S. Jennings, J. d. Oliverai, and K. J. Warr. Measurement of body size and abundance in tests of macroecological and food web theory. *Journal of Animal Ecology*, 76(1):72–82, 2007.

R. L. Lindeman. The trophic-dynamic aspect of ecology. *Ecology*, 23(4):399–417, 1942.

A. M. Makarieva, V. G. Gorshkov, B.-L. Li, S. L. Chown, P. B. Reich, and V. M. Gavrilov. Mean mass-specific metabolic rates are strikingly similar across life's major domains: evidence for life's metabolic optimum. *Proceedings of the National Academy of Sciences*, 105(44):16994–16999, 2008.

M. L. Pace, J. J. Cole, S. R. Carpenter, and J. F. Kitchell. Trophic cascades revealed in diverse ecosystems. *Trends in ecology & evolution*, 14(12):483–488, 1999.

J. H. Poelen, J. D. Simons, and C. J. Mungall. Global biotic interactions: an open infrastructure to share and analyze species-interaction datasets. *Ecological Informatics*, 24:148–159, 2014.

E. Sala and M. H. Graham. Community-wide distribution of predator–prey interaction strength in kelp forests. *Proceedings of the National Academy of Sciences*, 99(6):3678–3683, 2002.

R. Trebilco, J. K. Baum, A. K. Salomon, and N. K. Dulvy. Ecosystem ecology: size-based constraints on the pyramids of life. *Trends in ecology & evolution*, 28(7):423–431, 2013.

R. Trebilco, N. K. Dulvy, S. C. Anderson, and A. K. Salomon. The paradox of inverted biomass pyramids in kelp forest fish communities. *Proceedings of the Royal Society of London B: Biological Sciences*, 283(1833):20160816, 2016.

C. R. White and R. S. Seymour. Mammalian basal metabolic rate is proportional to body mass2/3. *Proceedings of the National Academy of Sciences*, 100(7):4046–4049, 2003.

C. B. Woodson, J. R. Schramski, and S. B. Joye. A unifying theory for top-heavy ecosystem structure in the ocean. *Nature communications*, 9(1):23, 2018.

Supporting Figures

We show in Fig. S1 the importance of using relative rather than absolute stability metrics, as the latter do not display clear patterns. Food chain stability and biomass patterns reported in the main text are more exhaustively mapped out in Fig. S2.

Figs. S3 to S6 provide more information about our empirical estimates of m. Fig. S4 compares empirical values of metabolic ratio m to predictions from body mass ratio $M^{1/4}$, showing significantly different patterns, and Fig. S7 shows that other parameters may depend on body size.

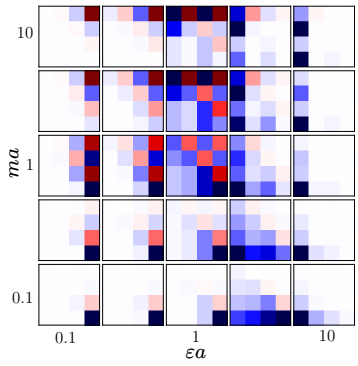

Figure S1: Absolute response ΔB_i to a press perturbation Δg_j. No clear pattern emerges here, due to being skewed by a changing biomass distribution. In Fig. S2, the symmetry with κ and the separation into pyramids and cascades becomes apparent when considering relative response $\Delta B_i/B_i$ to proportional perturbation $\Delta g_j/B_j$.

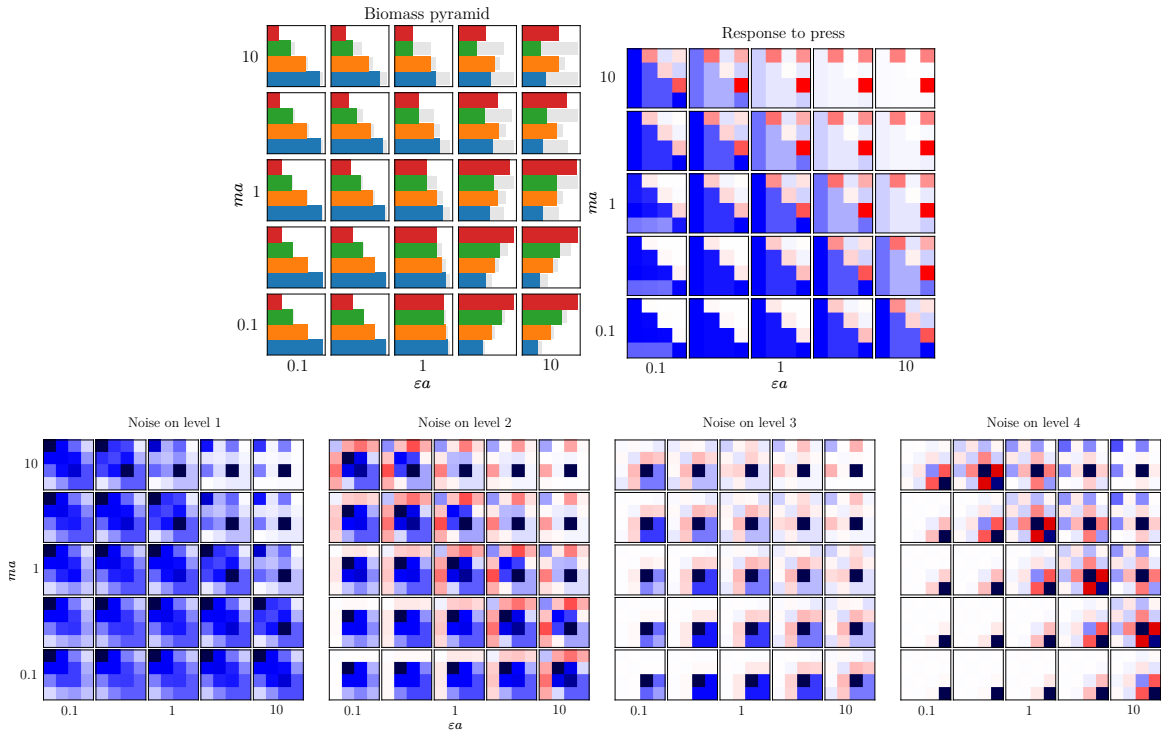

Figure S2: Exhaustive map of chain properties shown in Fig. 1 to 3. a) Biomass pyramids: the color bar shows the biomass per trophic level, the grey bar the biomass that would be reached without predation (allowing to estimate the importance of top-down control for each level). b) Relative response to a press perturbation. Blue represents a positive response (i.e. the response goes in the same direction as the perturbation) while red represents a negative or opposite response. An alternation of blue and red thus indicates a trophic cascade. c) Relative response to stochastic noise: adding noise on a given species, we can see the resulting covariance matrix between all the species. Blue represents positive covariance (variance is necessarily non-negative) and red represents negative covariance. An alternation of blue and red indicates a covariance cascade.

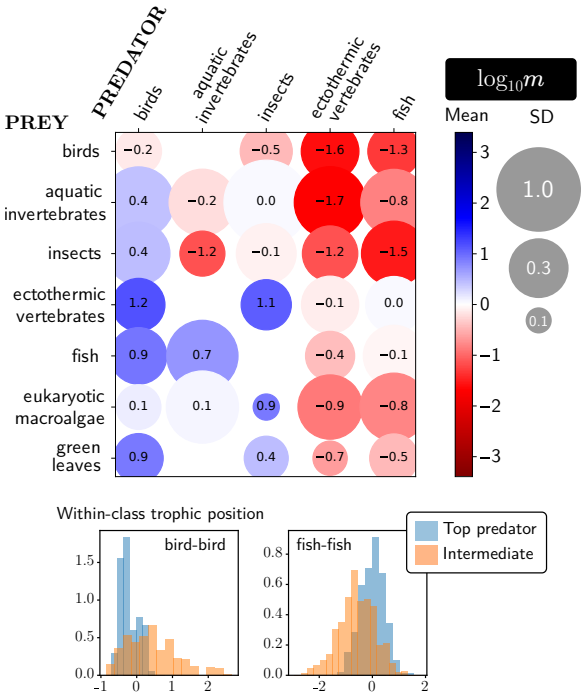

Figure S3: Empirical metabolic ratios m for various predator-prey pairs. Food chains can involve various types of organisms with different physiologies; therefore, the parameters held constant in (4) may in fact vary from link to link in the chain. We demonstrate this for m which varies over a large range $[10^{-2}, 10^{2}]$. We studied ∼12000 predator-prey pairs by matching extensive species metabolic data from Makarieva et al. [2008] with the Global Biotic Interactions (GloBI) database [Poelen et al., 2014] (see Supplementary Appendix). Colors and labels indicate mean values, while dot size indicates standard deviation. We find significant differences between large taxonomic classes: insect and bird predators tend to have faster metabolism than their prey, while aquatic organisms and terrestrial ectotherms tend to be slower (see also Fig. S5). In inset, we show differences between positions in tritrophic chains of species within the same class: intermediate predators exhibit much faster metabolism than their prey in the bird data, and much slower in the fish data, while top predators display a less skewed pattern in both. This data is used in Fig. 2 to estimate parameters in various ecosystems.

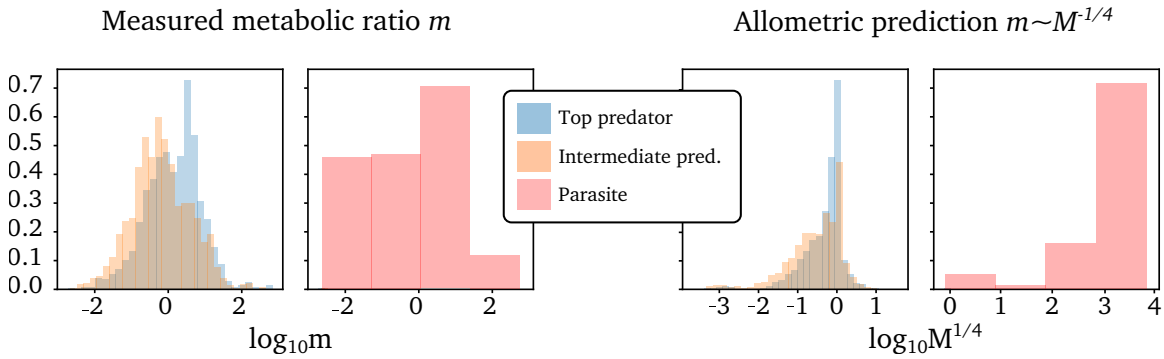

Figure S4: Empirical consumer-resource metabolic ratio $m = m_i/m_{i-1}$ and allometric predictions $M^{-1/4}$ with mass ratio $M = W_i/W_{i-1}$, derived from empirical measurements of m_i and W_i for in [Makarieva et al., 2008]. Every time, the ratio is measured from the perspective of the *consumer* i (see Fig. S5), and we distinguish different trophic positions for that consumer. We see that empirical measurements and scaling predictions present two starkly different pictures [Makarieva et al., 2008, Glazier, 2009]), especially by underestimating the occurrence of predators with faster metabolism $m > 1$ (red edges in the network). The allometric prediction $\log_{10} M^{-1/4}$ is strongly skewed toward the negative for predator-prey and the positive for parasite-host interactions, while empirical data shows no such skew. Body mass ratios also do not account fully for significant differences between top and intermediate predators.

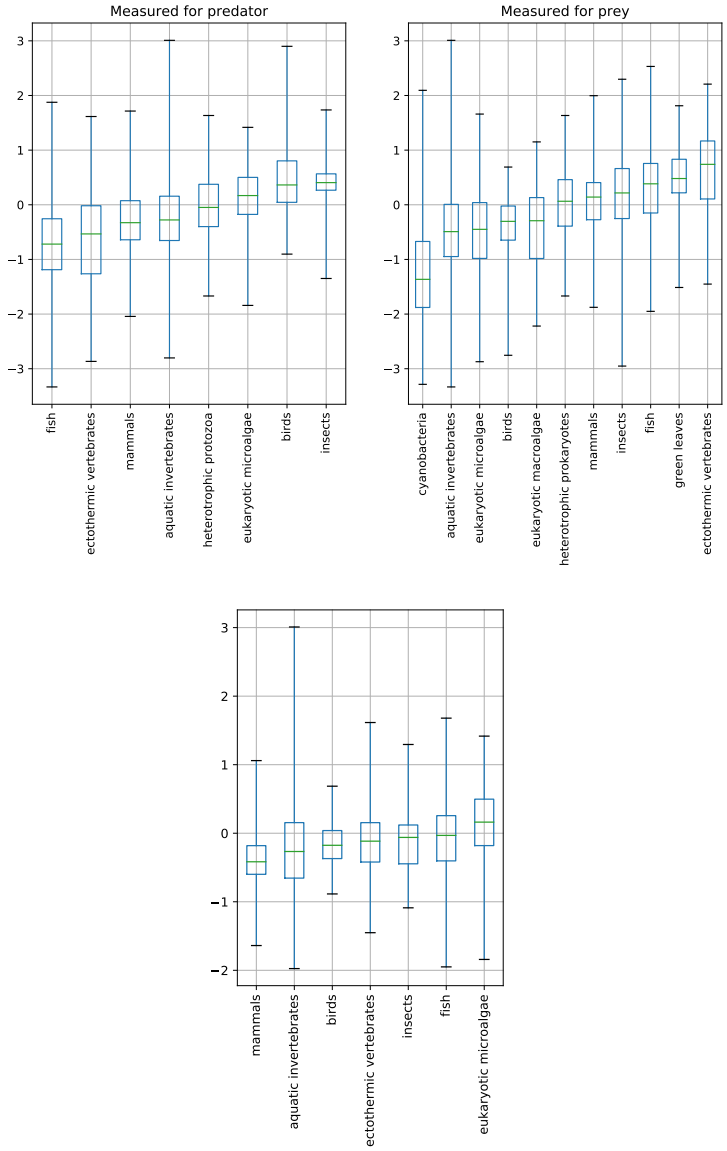

Figure S5: Distributions of m for various classes of organisms, measured either from the perspective of the predator or the prey,. The prey perspective corresponds more closely to the discussion in main text, as $m = m_{i+1}/m_i$ in the equations for the prey i throughout the text. The two perspectives tend to be anticorrelated: systematic differences between classes entail that, for instance, fish have globally lower metabolism and thus are the slower partner in a pair both when they are predators ($\log_{10} m < 0$, top-left panel) and when they are prey ($\log_{10} m > 0$, top-right panel). This issue disappears when considering only predator-prey pairs in the same class (bottom panel), although this necessarily skews the distribution in other ways (e.g. removing all classes that do not contain pairs).

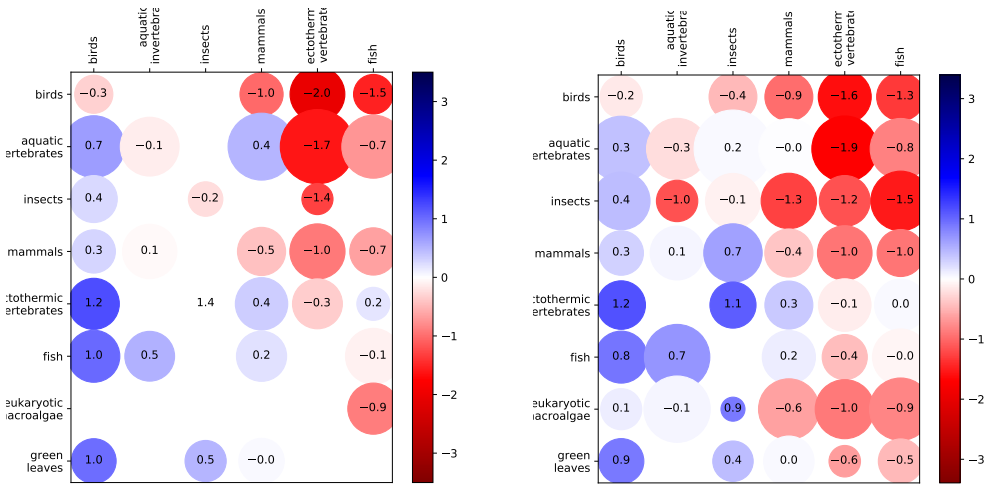

Figure S6: Results for distribution of $\log_{10} m$ (see Fig. S3) when retaining only exact species matches (left) versus genus matches (right). While the exact species matches retain much less information (1824 species pairs instead of 11822), statistics are fairly similar whenever they occur in both datasets, and this restriction does not affect our qualitative conclusions.

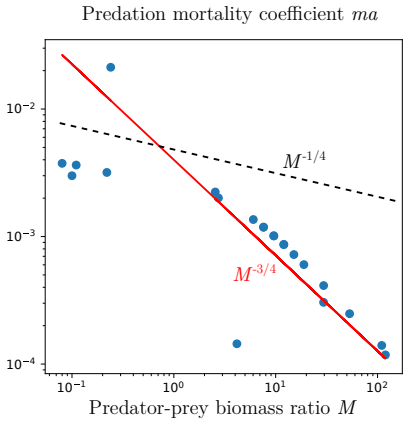

Figure S7: Strength of predation against predator-prey body mass ratio in herbivory in kelp forests. Data on per-capita predation mortality from Sala and Graham [Sala and Graham, 2002] was divided by predator body mass W to obtain the specific (per unit biomass) mortality coefficient, proportional to ma. The dashed line gives the metabolic prediction with constant interaction strength, $ma \sim M^{-1/4}$. The solid line is a guide for the eye, suggesting a much steeper scaling $ma \sim M^{-3/4}$ which would entail a fast decrease of the interaction strength (e.g. through the attack rate) with increasing body size ratio, $a \sim M^{-1/2}$.